Plasma-sprayed zirconia bond coat as an intermediate layer for hydroxyapatite coating on titanium alloy substrate

BANG-YEN CHOU, EDWARD CHANG*
Department of Materials Science and Engineering, National Cheng Kung University, Tainan, Taiwan 701

This study aims to strengthen the bonding at HA coating/Ti–6Al–4V interface by adding an intermediate ZrO_2 bond coat between them. The bonding strength of the HA/ZrO_2 coating was evaluated with the separately prepared HA coating as control. The phase, microstructure and chemistry, and surface roughness of the plasma-sprayed two-layer HA/ZrO_2 coating on Ti–6A1–4V substrate were investigated by X-ray diffractometry, scanning electron microscopy, and surfcorder, respectively. Experimental results indicate that the bonding strength increases from 28.6 ± 3.22 MPa for HA coating to 36.2 ± 3.02 MPa for HA/ZrO_2 composite coating. Elemental analysis employed on the surface of ZrO_2 bond coat, on which the HA top coat was first dissolved completely in HCl acid, reveals the sign of diffusion of calcium ions from HA to ZrO_2 bond coat. In addition, rougher surface morphology provided by ZrO_2 bond coat is also considered to aid in the bonding at HA/ZrO_2 interface. Similar coating system done by other researchers is compared and discussed.

1. Introduction

Due to its biocompatibility, hydroxyapatite ($Ca_{10}(PO_4)_6(OH)_2$, HA) has attracted wide interest as a potential structural ceramic material for biological implants [1, 2]. One of the major disadvantages of this material is the rather low fracture strength and low fracture toughness, i.e. its high brittleness [3–5]. This results in a strong limitation of the potential application of HA as a replacement for human bones since it could easily fail under load.

Plasma-sprayed HA-coated Ti alloy, exhibiting both excellent biocompatibility and satisfactory mechanical properties, is more suitable for surgical implants [6–8]. Most previous studies addressing the biological and biomechanical behaviors at HA coating/bone interface have shown encouraging results. However, in evaluating the performance and stability of HA coating in the load-bearing situation after long-term follow-up, special consideration should be given to the HA coating/Ti alloy interface. Despite a possible chemical bond observed at HA coating/Ti alloy substrate [9–10], researches suggest the presence of a potentially weak HA coating/Ti alloy interface [9, 11–14], which may compromise the function of the implant devices. It was reported by Spivak *et al*. [13] that the failure of HA coating/Ti/bone specimen under tensile testing occurred consistently at HA coating/Ti interface, indicating clearly that the interface bonding was not strong enough to reach a reliable requirement. Using a modified short-bar technique for interfacial fracture toughness determination, Filiaggi *et al*. [9] showed in another study that there existed relatively low fracture toughness values in the HA-coated Ti–6Al–4V implant. Therefore, concerns should be paid in the promotion of bonding at HA coating/Ti alloy interface.

Some improvements have been suggested for enhancing the HA coating/Ti alloy bonding. These may be achieved by, (1) a denser HA coating (less porosity) [15]; (2) a thinner HA coating (50–75 μm), which reduces the internal stress and enhances the cohesive strength in the interlamellar structure [15, 16]; (3) a post-heat treatment of HA coating *in vacuo* after plasma spraying, which would promote the formation of a titanium-phosphate compound at the interface [17]. However, the above improvements are accompanied by some disadvantages, for instances: (1) a denser microstructure usually means more amorphous phases existed in plasma-sprayed HA coating; (2) a thinner HA coating may not be thick enough to tolerate the initial *in vivo* biodegradation; (3) a high temperature heat treatment usually causes the Ti alloy to lose its strength.

In this study, efforts were paid to strengthen the interface bonding by adding an intermediate coating (ZrO_2 bond coat) between HA coating and Ti alloy substrate, since ZrO_2 is well known for its high mechanical strength, fracture toughness, and usually used to strengthen other ceramics [18, 19]. This work aims to study the bonding strength and strengthen

*Author to whom all correspondence should be addressed.

mechanisms of plasma-sprayed two-layer HA/ZrO_2 composite coating on the Ti alloy substrate, using pure HA coating as control.

2. Materials and methods

2.1. Powder and specimen preparations

Hydroxyapatite powder (HA powder, typical size 7.0 μm) and ZrO_2 powder stabilized with 8 mol % Y_2O_3 (TZ8Y powder, typical size 0.2 μm) were obtained from the commercial products of Merck and TOSOH, respectively. Both HA and ZrO_2 powders were granulated with 10 wt % of aqueous PVA solution (conc. at 5 wt %), sieved to mesh No. +120 to −80 (125–177 μm) and heated at 600 °C for 1 h to volatilize the PVA binder, then sintered at 1000 °C for 4 h to consolidate the particles.

As-sintered ZrO_2 powder was first coated by plasma-spraying deposition onto the Al_2O_3 grit-blasted substrate of standard Ti–6Al–4V titanium alloy (ASTM F-136); then, as-sintered HA powder was applied as top coat onto the intermediate ZrO_2 bond coat. The thickness of ZrO_2 bond coat was 15 μm and the total thickness of HA/ZrO_2 coating was 150 μm. During plasma-spraying deposition, powers of 42 KW and 40.2 KW were employed for ZrO_2 bond coat and HA top coat, respectively, where both primary gas of argon and secondary gas of hydrogen were used.

2.2. Material characterization

Plates of Ti–6Al–4V alloy (100 mm × 25 mm × 3 mm) coated with sole ZrO_2 bond coat or two-layer HA/ZrO_2 composite coating thereon were both prepared for X-ray diffraction (XRD) and scanning electron microscopy (SEM) analysis. For XRD analysis, the phase identity of both ZrO_2 bond coat and HA top coat was examined by Rigaku D/MAX III.V with CuK_α radiation, operated at 30 KV, 20 mA and scan speed of 1°/min. For SEM investigation, the morphology of powder, coating surface, cross-sectional microstructure and chemistry analysis were examined by Philips XL-40 FEG. Thereafter, the surface roughness of grit-blasted Ti–6A1–4V alloy and ZrO_2 bond coat were evaluated by surfcorder SE-40D, Kosaka Laboratory Ltd.

2.3. Bonding strength testing

Rods of Ti–6Al–4V alloy with 1 inch diameter were used for the measurement of the bonding strength of the coating per ASTM C633-79. For specimen preparation, end surface of one rod was first roughened by Al_2O_3, grit-blasted and then plasma-sprayed depositing the desired HA/ZrO_2 coating or pure HA coating thereon. The nominal thickness of coating was 150 μm. End surface of another coupling rod was also grit-blasted and adhered to the corresponding surface of HA/ZrO_2 or pure HA coating with a thermoplastic glue (METCO EP-15). The adhesive and curing process of the couples were done under pressure in a fixture at 190 °C for 2 h. The couples were then subjected to tensile tests at a constant cross-head speed of 0.02 mm/s until failure. The fracture surface was examined by optical microscope (OM). For each testing material, ten specimens were used, and the bonding strength data were reported as the average values.

3. Results

3.1. Characterization of powder

The powders of HA and ZrO_2 ready for plasma spraying are characterized by their morphology and phase contents. XRD spectra of the original and as-sintered HA powders are shown in Fig. 1. Similar X-ray diffraction analysis is also applied to the original and as-sintered ZrO_2 powders as shown in Fig. 2. From the comparison of Fig. 1(a) and (b), it is seen that a well crystalline HA powder ready for plasma spraying is obtained after the sintering and consolidating processes, while the decomposition of HA is not observed. Also there is no phase change in ZrO_2 powder after the consolidating process based on the XRD results of Fig. 2.

The morphologies of as-sintered powders of HA and ZrO_2 consisting of aggregates of particles are shown in Fig. 3(a) and (b), respectively. Sintering of HA particles is evident, while the extent of sintering for ZrO_2 particles seems to be much less than that of the former.

3.2. Bonding strength measurements

The bonding strength data measured from the adhesion test per ASTM C633-79 are listed in Table I, where each value in the table represents an average of ten test data. It

TABLE I Results of bonding strength measurements

Coatings	Bonding strength (MPa)
HA coating	28.6 ± 3.22
HA coating with ZrO_2 bond coat	36.2 ± 3.02

Values are given as mean ± SD from ten tests.

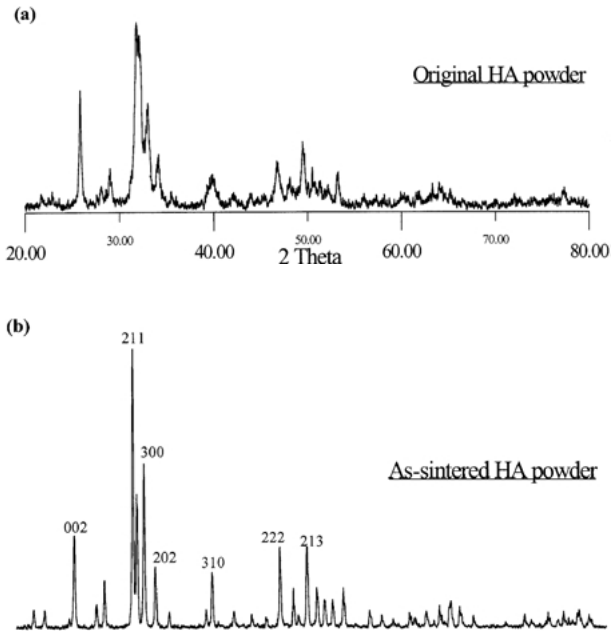

Figure 1 XRD patterns of, (a) original HA powder, and (b) as-sintered HA powder.

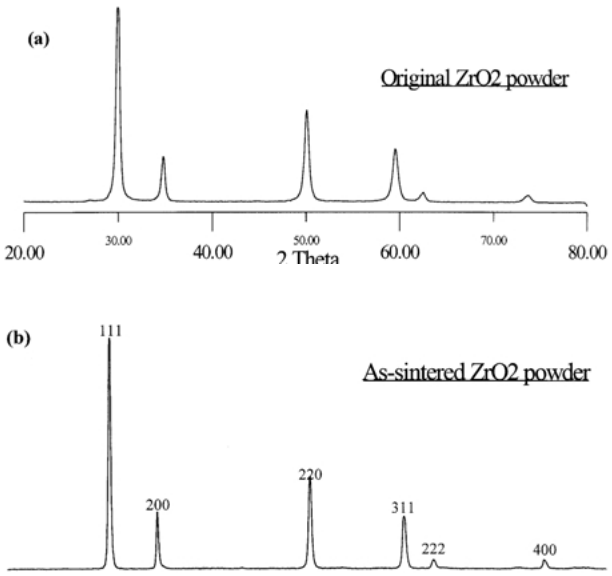

Figure 2 XRD patterns of, (a) original ZrO_2 powder, and (b) as-sintered ZrO_2 powder.

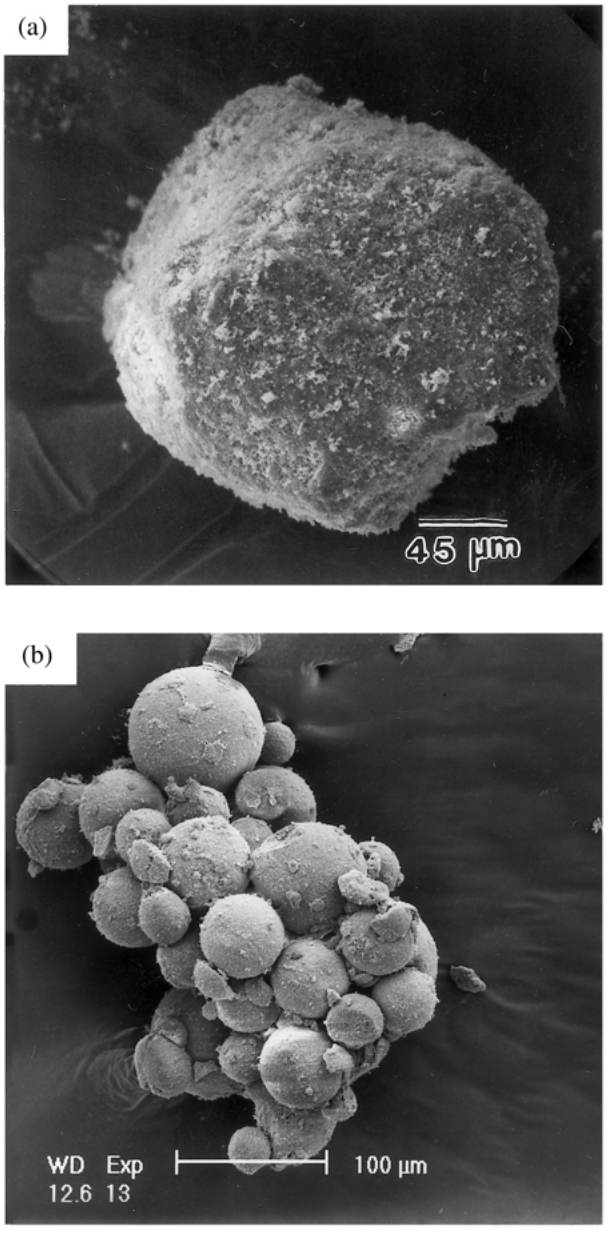

Figure 3 SEM surface morphologies of, (a) as-sintered HA powder, and (b) as-sintered ZrO_2 powder.

TABLE II Results of surface roughness measurements

Surface roughness (Ra)	
Grit-blasted Ti–6A1–4V substrate	3.55
ZrO_2 bond coat	5.73
HA coating without ZrO_2 bond coat	9.44
HA coating without ZrO_2 bond coat	10.20

Values are averages of ten test data.

is found that the bonding strength increases from 28.6 ± 3.22 MPa (mean $\pm$ SD) for HA coating to 36.2 ± 3.02 MPa for HA/ZrO_2 composite coating.

3.3. Characterization of coating

The results of surface roughness measurement for grit-blasted Ti–6A1–4V substrate, ZrO_2 bond coat, and HA coating with or without ZrO_2 bond coat are summarized in Table II. The values displayed in Table II are measurements from averages of ten test data. The surface roughness of ZrO_2 bond coat is 5.73 μm (Ra), while that of grit-blasted Ti–6A1–4V substrate is only 3.55 μm (Ra). The ZrO_2 bond coat provides a rougher surface for the deposition of HA compared with the As grit-blasted Ti–6A1–4V. Consequently, the topography of HA coating with the ZrO_2 bond coat exhibits a higher surface roughness value (10.2 μm) than that of HA coating without the ZrO_2 bond coat (9.44 μm).

Fig. 4(a) and (b) show the XRD results of as-sprayed ZrO_2 bond coat and HA top coat. The appearance of Ti (1 0 1) and (0 0 2) peaks in XRD spectrum of Fig. 4(a) is caused by the penetrating X-ray beam through the thin layer of ZrO_2 and reaching the Ti alloy substrate. Traces of α-calcium phosphate (α-TCP), tetracalcium phosphate (TP) and CaO are present in HA coating as shown in Fig. 4(b).

The surface morphologies observed by SEM of the grit-blasted Ti–6A1–4V substrate, as-sprayed ZrO_2 bond coat and HA top coat are shown in Fig. 5. SEM cross-

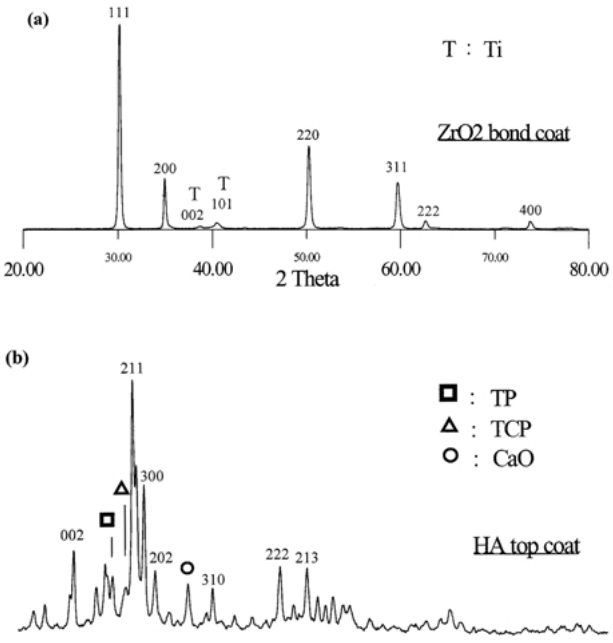

Figure 4 XRD patterns of as-sprayed, (a) ZrO_2 bond coat, and (b) HA top coat.

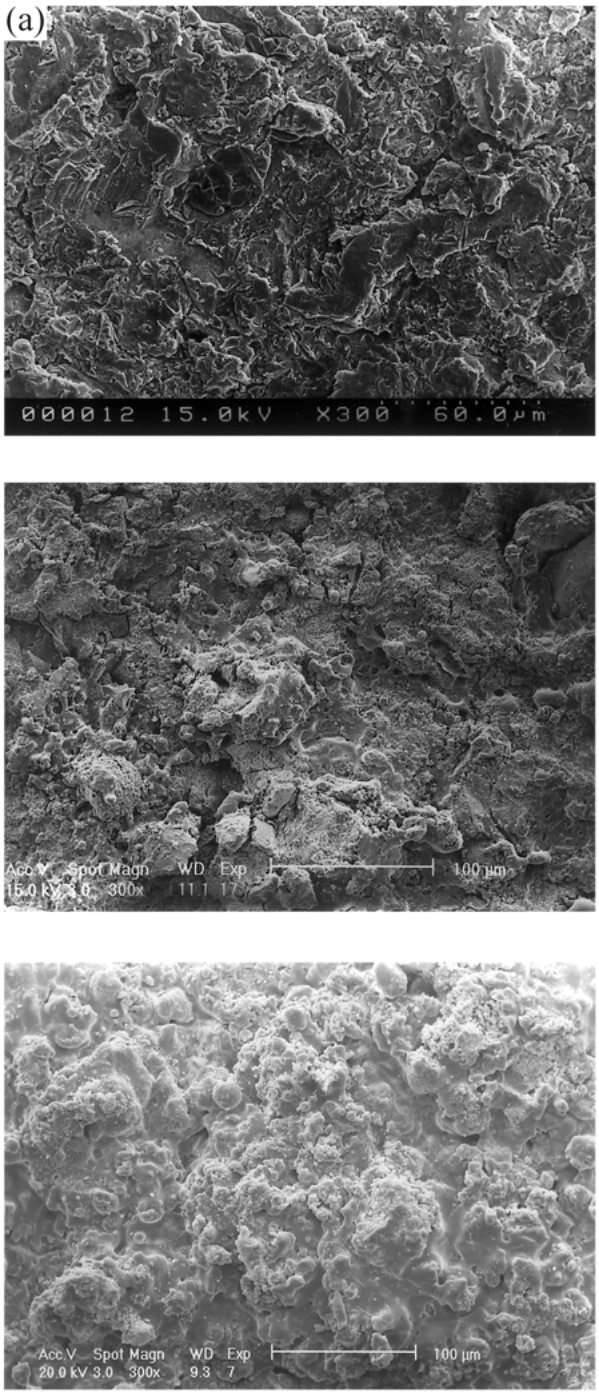

Figure 5 SEM surface morphologies of, (a) Al_2O_3 grit-blasted Ti–6A1–4V substrate, (b) as-sprayed ZrO_2 bond coat, and (c) as-sprayed HA top coat.

sectional view of the two-layer HA/ZrO_2 coating on Ti–6A1–4V substrate is shown in Fig. 6, where EDS line scan indicates the corresponding Ca element distribution.

4. Discussion

For clinical application of HA coated Ti–6A1–4V implant with satisfactory long-term fixation to bone, the bonding strength at HA coating/Ti–6A1–4V interface should be as high as possible. There is evidence of a potentially weak HA coating/Ti alloy interface from the observation of failure mode, occurred consistently at HA coating/Ti alloy interface, under tensile testing [13]. The inherent pore and crack in the lamellar structure of coating are detrimental to the adhesion of HA to metal

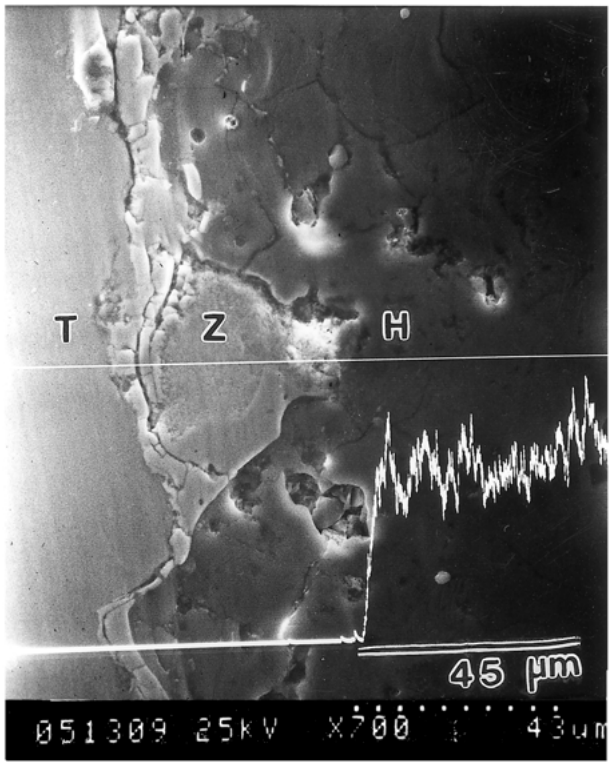

Figure 6 SEM cross-sectional microstructure of plasma-sprayed two-layer HA/ZrO_2 coating with EDS line scan of Ca element distribution. T, Z, and H denote Ti alloy, ZrO_2, and HA, respectively.

substrate and hence the fixation of HA-coated implant with bone [15, 20]. Nevertheless, the pores adjacent to the surface of HA coating are considered to aid in the osteoconductivity by enhancing tissue ingrowth into them [21]. Moreover, in spite of the existence of pore and crack in the lamellar structure of HA coating, it is found from an *in vitro* immersion test that the HA coating can retard the release of metal ions effectively from the metal substrate [22, 23]; the data indicate that HA coating with a thickness of only 50 µm is sufficient to act as a barrier. With the increasing porosity content and thickness of HA coating, the HA coating and the bonding at HA coating/Ti alloy interface is undermined. This study aims to strengthen the HA coating/Ti alloy interface by furnishing a bond coat interlayer of zirconia which might provide a mechanical interlocking and chemical bond between the HA coating and the bond coat.

The SEM surface of ZrO_2 bond coat (Fig. 5(b)) is evidently rougher than the surface morphology of as grit-blasted Ti–6A1–4V substrate (Fig. 5(a)). The observation seems to be in consistence with the measured values of surface roughness listed in Table II. In the study by Filiaggi *et al*. [9], lower fracture toughness and bonding strength were reported to correlate with lower surface roughness of the Ti–6A1–4V substrate. Hence, the rougher surface provided by ZrO_2 bond coat is thought to be one of the strengthening mechanisms which contribute to the performance of HA/ZrO_2 coating system. In addition, it is noted that the surface roughness of HA coating with a ZrO_2 bond coat is higher than the one without (Table II). This is obviously caused by the rougher ZrO_2 bond coat as an intermediate layer for the top coating of HA. Because of the granulated process for the preparation of ZrO_2 powder ready for

(b)

Untitled: 1

Label: normal

kV: 20.0	Tilt: 0.0	Take-off: 35.7	Det Type: SUTW+	Res: 134	Tc: 40
FS : 765	Lsec : 87			10-Jun-99	10:47:23

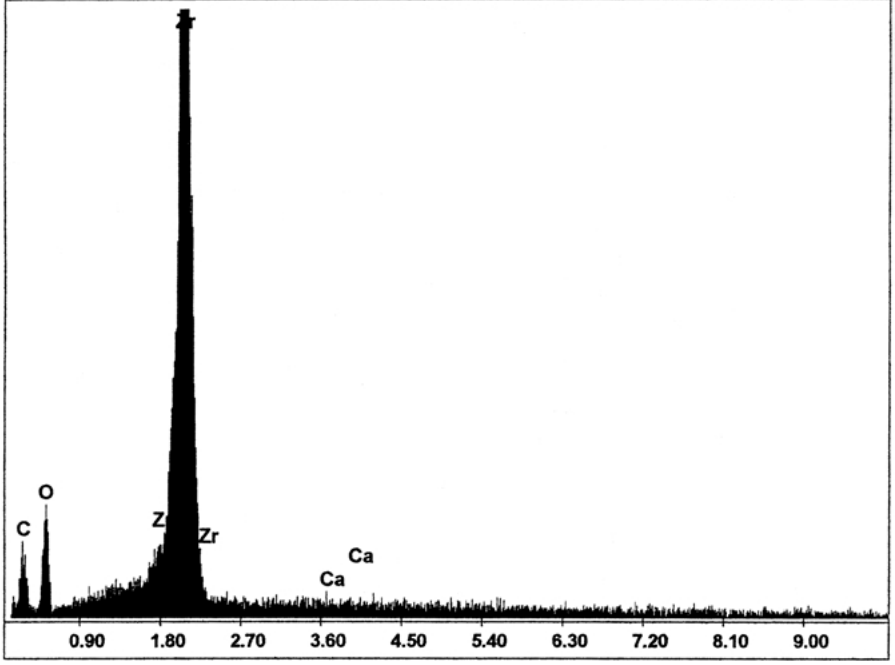

Element	Wt %	At %	K-Ratio	Z	A	F
ZrL	99.71	99.33	0.9964	0.9993	1.0000	1.0000
CaK	0.29	0.67	0.0023	1.1913	0.6672	1.0000
Total	100.00	100.00				

Figure 7 (a) SEM microstructure of ZrO_2 bond coat, on which the HA top coat of HA/ZrO_2 coating is dissolved in HCl acid. (b) EDS chemical analysis and semi-quantitative calculation of the local area as shown in (a).

plasma spraying, the plasma-sprayed ZrO_2 bond coat reveals a distinctive SEM cross-sectional microstructure of HA/ZrO_2 coating (Fig. 6). The apophyses as shown in Fig. 6 have contributed to the increase of surface roughness and surface area provided for the subsequent deposition of HA. In addition, since the apophyses structure of ZrO_2 bond coat should serve as anchorage of HA top coat, the toughness of ZrO_2 is likely to play a role in the bonding strength performance. Although it still needs extra work to gain further evidences, the toughness of ZrO_2 has presumably been considered to aid in the whole bonging strength.

The phase content of as-sintered HA powder (Fig. 1(b)) has changed in HA coating (Fig. 4(b)) by the appearance of trace phases, such as α-TCP, TP and CaO. These traces are the products of the decomposition of HA during plasma spraying and the results are consistent with the literature [24, 25]. Nevertheless, it is seen that the phase content of ZrO_2 bond coat is not changed after plasma spraying by the comparison of XRD spectra of

as-sintered ZrO_2 powder (Fig. 2(b)) and ZrO_2 bond coat (Fig. 4(a)). The choice of ZrO_2 as material of bond coat in the present study is based on the results of previous studies [26, 27] concerning the incorporation of ZrO_2 particles in reinforcing plasma-sprayed HA coating on Ti–6A1–4V substrate. Some of the conclusions are stated as follows: (1) The crystal structure of the ZrO_2 powder used in the studies is stable in cubic phase after plasma spraying. (2) After plasma spraying, examination of microstructural investigation reveals that the ZrO_2 particles embedded in HA matrix exhibit a good interfacial contact with the matrix. (3) Diffusion of calcium ions from the HA matrix into the interior of ZrO_2 crystal is evident and the transport could further improve the interfacial property.

Whether the diffusion of calcium ions from HA top coat into ZrO_2 bond coat occurs during the deposition of HA is unknown in the present study. Fig. 7(a) shows the SEM microstructure of ZrO_2 bond coat, on which the HA top coat of HA/ZrO_2 composite coating has been completely dissolved in HCl acid. The corresponding semi-quantitative analysis of energy-dispersive spectrum (EDS) from this area (Fig. 7(b)) indicates the existence of trace Ca on the specimen. The preliminary result from the semi-quantitative analysis suggests a possible diffusion of calcium ions from HA to ZrO_2 bond coat. Confirmation of the diffusion of calcium ions should be further investigated by the technique of transmission electron microscopy (TEM). Consequently, the ZrO_2 bond coat fabricated by the method in the present study could possibly form a diffusion bonding with the HA top coat and hence further strengthen the HA/ZrO_2 coating.

Kurzweg *et al*. [28] reported an enhanced plasma-sprayed HA coating on Ti–6A1–4V substrate by introducing TiO_2 and ZrO_2 as bond coat between HA coating and metal substrate. In the study [28], HA coating with ZrO_2 bond coat underlying has the worst performance in terms of the *in vitro* resorption resistance and the peel adhesion test. On the other hand, HA coatings with $(TiO_2 + ZrO_2)$ bond coat or pure TiO_2 bond coat possess improved coatings performance. It is apparent that the results of performance from the present HA/ZrO_2 coating system are inconsistent with that of Kurzweg *et al*. The possible reasons are: (1) The ZrO_2 powder ready for plasma spraying is obtained from a granulated process with a size distribution of $125 \sim 177\,\mu m$ in our present study. The purpose of the granulated process for ZrO_2 powder is to fabricate a plasma-sprayed ZrO_2 bond coat with surface roughness as high as possible than that of the grit-blasted Ti–6A1–4V substrate. The performance of coating has been reported to correlate with the roughness of the deposited surface [9]. Nevertheless, the ZrO_2 powder used in Kurzweg *et al*.'s study [28] was probably not granulated and the surface roughness of the bond coat was neglected. (2) In Kurzweg *et al*.'s study [28], the massive copper block used in ASTM D3167-76 peel test [29], acts as a heat sink. The heat sink may exert a different effect on the hydroxyapatite/ZrO_2 bond coat system as compared to the other coating systems in their study [28]; the reason is that ZrO_2 is a well-known thermal insulative material. (3) Fully-stabilized ZrO_2 powder is used in our present study, but the one used in Kurzweg *et al*.'s study [28] is partially stabilized. Positive results were also obtained by Matejka [30] who used stabilized ZrO_2 bond coats to improve the HA/ZrO_2 coating systems.

5. Conclusions

1. Two-layer HA/ZrO_2 composite coating can be fabricated by plasma spraying. The bonding in HA coating/Ti–6Al–4V interface can be strengthened by introducing a ZrO_2 bond coat between them. The bonding strength increases from 28.6 ± 3.22 MPa for HA coating to 36.2 ± 3.02 MPa for HA/ZrO_2 composite coating.

2. The possible strengthening mechanisms in HA/ZrO_2 composite coating are summarized as follows: (a) Rougher surface provided by ZrO_2 coat promotes mechanical interlocking between HA and ZrO_2. The surface morphology of ZrO_2 bond coat with apophyses thereon promotes the bonding strength by the increase of surface area. In addition, the toughness of ZrO_2 could play a role in the strengthening. (b) Preliminary study indicates the sign of interdiffusion of elements between HA and ZrO_2, which is likely to promote a better interface bonding.

References

1. A. RAVAGLIOLI and A. KRAJEWSKI, ''Bioceramics: Materials, Properties, Applications'' (Chapman and Hall, London, UK, 1992).
2. L. L. HENCH, in ''Annals of the New York Academy of Sciences'', edited by P. Ducheyne and J. E. Lemons (New York Academy of Sciences, New York, 1988) pp. 54–71.
3. R. I. MARTIN and P. W. BROWN, *J. Mater. Sci.: Mater. Med.* **6** (1995) 138.
4. N. YAMASAKI, K. YANAGISAWA and N. KAKIUCHI, *J. Mater. Res.* **5** (1990) 647.
5. N. YAMASAKI, T. KAI, N. NISHIOKA, K. YANAGISAWA and K. IOKU, *J. Mater. Sci. Lett.* **9** (1990) 1150.
6. B. C. WANG, E. CHANG and C. Y. YANG, *J. Biomed. Mater. Res.* **27** (1993) 1315.
7. B. C. WANG, E. CHANG, D. TU and C. Y. YANG, *J. Mater. Sci. Mater. Med.* **4** (1993) 394.
8. M. GOTTLANDER and T. ALBREKTSSON, *Int. J. Oral Maxillofac. Imp.* **6** (1991) 339.
9. M. J. FILIAGGI, N. A. COOMBS and R. M. PILLIAR, *J. Biomed. Mater. Res.* **25** (1991) 1211.
10. H. JI. C. B. PONTON and P. M. MARQUIS, *J. Mater. Sci. Mater. Med.* **3** (1992) 283.
11. M. L. FILIAGGI, N. A. COOMBS and R. M. PILLIAR, *Mater. Res. Soc. Symp. Proc.* **153** (1989) 377.
12. R. M. PILLIAR, D. A. DEPORTER, P. A. WATSON, M. PHAROAH, M. CHIIPMAN, N. VALIQUETTE, S. CARTER and K. DE GROOT, *J. Dent. Res.* **70** (1991) 1338.
13. J. M. SPIVAK, J. L. RICCI, N. C. BLUMENTHAL and H. ALEXANDER, *J. Biomed. Mater. Res.* **24** (1990) 1121.
14. S. D. COOK, J. F. KAY, K. A. THOMAS and M. JARCHO, *Int. J. Oral Maxillofac. Imp.* **2** (1987) 15.
15. B. C. WANG, E. CHANG, C. Y. YANG, D. TU and C. H. TASI, *Surf. Coat. Technol.* **58** (1993) 107.
16. E. MUNTING, M. VERHELPEN, F. LI and A. VIACENT in ''CRC Handbook of Bioactive Ceramics'', edited by T. Yamamuro, L. L. Hench and J. Wilson (CRC Press, Florida, 1990) pp. 143–148.
17. H. JI and P. M. MARQUIS, *Biomaterials* **14** (1993) 64.
18. D. J. GREEN, *J. Am. Ceram. Soc.* **65** (1982) 610.
19. M. RUHLE, A. G. EVANS, R. M. MCMEENING and P. G. CHARALAMBIDES, *Acta Metall.* **35** (1987) 2701.

20. J. ILAVSKY, A. J. ALLLEN, G. G. LONG, S. KRUEGER, C. C. BERNDT and H. HERMAN, *J. Am. Ceram. Soc.* **80**(3) (1997) 733.
21. S. D. COOK, K. A. THOMAS, J. F. KAY and M. JARCHO, *Clin. Orthop.* **230** (1988) 303.
22. S. R. SOUSA and M. A. BARBOSA, *Biomaterials* **17**(4) (1996) 397.
23. S. R. SOUSA and M. A. BARBOSA, *J. Mater. Sci.: Mater. Med.* **6**(12) (1995) 818.
24. G. DE WITH, H. J. A. VANDIJK, N. HATTU and K. PRIJS, *J. Mater. Sci.* **16** (1981) 1592.
25. M. B. THOMAS, R. H. DOREMUS, M. JARCHO and R. L. SALSBURY, *J. Mater. Sci.* **15** (1980) 891.
26. BANG-YEN CHOU and EDWARD CHANG, *Biomaterials* **20** (1999) 1823.
27. BANG-YEN CHOU, EDWARD CHANG, SHYUE YEN YAO and JEN MIN CHEN, *J. Am. Ceram. Soc.*
28. H. KURZWEG, R. B. HEIMANN, T. TROCZYNSKI and M. L. WAYMAN, *Biomaterials* **19** (1998) 1507.
29. M. SEXSMITH and T. TROCZYNSKI, *J. Thermal Spray Technol.* **3** (1994) 404.
30. D. MATEJKA, V. PALKA and I. INFNER, in ''IV. Work-shop Plasmatechnik'', edited by G. Nutsch, 14–15 October 1996 (TU, Ilmenau, 1996).

Received 21 July 2000
and accepted 27 July 2001